NIH Public Access
Author Manuscript
Dev Dyn. Author manuscript; available in PMC 2014 June 08.

Published in final edited form as:
Dev Dyn. 2012 August ; 241(8): 1310–1324. doi:10.1002/dvdy.23812.

Biallelic expression of *Tbx1* protects the embryo against developmental defects caused by increased Receptor Tyrosine Kinase signalling

Subreena Simrick[1,^], **Dorota Szumska**[2], **Jennifer R. Gardiner**[1,$], **Kieran Jones**[1], **Karun Sagar**[1], **Bernice Morrow**[3], **Shoumo Bhattacharya**[2], and **M. Albert Basson**[1,*]

[1] Department of Craniofacial Development and Stem Cell Biology, King's College London, 27th floor, Guy's Tower, London SE1 9RT, UK

[2] The Wellcome Trust Centre for Human Genetics, Roosevelt Drive, Oxford, OX3 7BN, UK

[3] Department of Molecular Genetics, Albert Einstein College of Medicine, 1301 Morris Park Avenue, Price Center Room 402, Bronx, NY 10461, USA

Abstract

Background—22q11.2 deletion syndrome (22q11DS) is the most common microdeletion syndrome in humans, characterised by cardiovascular defects such as interrupted aortic arch, outflow tract defects, thymus and parathyroid hypo- or aplasia and cleft palate. Heterozygosity of *Tbx1*, the mouse homologue of the candidate *TBX1* gene, results in mild defects dependent on genetic background, whereas complete inactivation results in severe malformations in multiple tissues.

Results—The loss of function mutations in two Sprouty genes, which encode feedback antagonists of receptor tyrosine kinase (RTK) signaling, phenocopy many defects associated with the syndrome in the mouse. The stepwise reduction of Sprouty gene dosage resulted in different phenotypes emerging at specific steps, suggesting that the threshold up to which a given developmental process can tolerate increased RTK signaling is different. *Tbx1* heterozygosity significantly exacerbated the severity of all these defects, which correlated with a substantial increase in RTK signaling.

Conclusions—Our findings suggest that TBX1 functions as an essential component of a mechanism that protects the embryo against perturbations in RTK signaling that may lead to developmental defects characteristic of 22q11.2 deletion syndrome. We propose that genetic factors that enhance RTK signalling ought to be considered as potential genetic modifiers of this syndrome.

[*]Corresponding author: Dr. M. A. Basson, Department of Craniofacial Development and Stem Cell Biology, King's College London, Floor 27, Guy's Tower, London SE1 9RT, UK Tel: +44 (0)207 188 1804 Fax: +44(0)207 188 1674 albert.basson@kcl.ac.uk.
[^]Current address: Heart Science Centre, Imperial College London, Harefield, UK
[$]Current address: Department of Cancer Biology, Institute of Cancer Research, 123 Old Brompton Road, London SW7 3RP, UK

NIH-PA Author Manuscript
NIH-PA Author Manuscript
NIH-PA Author Manuscript

NIH-PA Author Manuscript
NIH-PA Author Manuscript
NIH-PA Author Manuscript

Introduction

22q11.2 deletion syndrome (22q11DS), also referred to as DiGeorge syndrome/velocardio-facial syndrome (DGS/VCFS) is characterized by a range of defects, that include congenital heart disease, palate anomalies, hypocalcaemia, T cell mediated immunodeficiency, cognitive difficulties, and dysmorphic faces (Frank et al., 2002). Cardiovascular anomalies include interrupted aortic arch type B (IAA-B) and other aortic arch defects, persistant truncus arteriosus, tetralogy of Fallot and ventricular septal defects (VSD). Most 22q11DS features appear to be due to defects during development of a transient structure in the midgestation embryo, the pharyngeal apparatus (Baldini, 2005; Wurdak et al., 2006). Human genetic studies have shown that 22q11DS is most often associated with a 3Mb microdeletion at chromosome 22q11.2, occurring in approximately 1/4000 births, making it the most common microdeletion syndrome (Scambler, 2000; Botto et al., 2003; Kobrynski and Sullivan, 2007). Some 22q11DS patients have a smaller, nested distal deletion endpoint resulting in a 1.5 Mb deletion (McDermid and Morrow, 2002). Genetic studies in the mouse have shown that haploinsufficiency or complete loss of *Tbx1*, within the 1.5 Mb region, can recapitulate most of the physical anomalies. 22q11DS patients with mutations in *TBX1* in the absence of 22q11 microdeletions have been identified, confirming *TBX1* as a prime candidate gene for the syndrome (Gong et al., 2001; Yagi et al., 2003; Zweier et al., 2007). Another gene outside the 1.5 Mb interval, *Crkl*, which encodes an intracellular RTK signaling adaptor, may modify the phenotype, because inactivation of *Crkl* results in similar thymus and cardiovascular anomalies in the mouse. These studies have confirmed that combined heterozygosity for *Tbx1* and *Crkl* significantly exacerbated the phenotypes associated with either *Tbx1* or *Crkl* heterozygosity (Guris et al., 2006). These and other studies have indicated that the level of TBX1 is critical for normal development and factors that can alter the intensity of signalling pathways sensitive to TBX1 dosage are of particular interest in understanding the severity of disease.

Indeed, the large clinical variability that typifies this syndrome suggests that factors outside the typically deleted region may modify the phenotype. In order to fully understand this disease, it is vital that these modifiers are identified. Potential modifying mechanisms include differences in breakpoints during deletion, specific modifier genes outside the critical region, allelic variation of genes within the critical region on the non-deleted chromosome, epigenetic phenomena and environmental factors (Scambler et al., 1991; Morrow et al., 1995; Carlson et al., 1997). The search for modifier genes in patients have so far met with limited success (Driscoll et al., 2006; Goldmuntz et al., 2009). Studies in mouse embryos have suggested that *Tbx1* functions in a genetic pathway upstream of Fibroblast Growth Factor (FGF) signaling (Abu-Issa et al., 2002; Frank et al., 2002; Vitelli et al., 2002; Brown et al., 2004; Arnold et al., 2006b; Park et al., 2006). Accordingly, loss of function mutations in genes encoding FGF ligands can enhance the mild phenotypes in *Tbx1*+/- mutants (Vitelli et al., 2002; Aggarwal et al., 2006). Similarly, variants of the Vascular Endothelial Growth Factor (*Vegf*) gene have been identified as a potential modifier of the pharyngeal arch artery phenotype in mice and humans (Stalmans et al., 2003). A number of other genes have been found to genetically interact with *Tbx1* during mouse development, including the BMP antagonist, Chordin, the cardiac transcription factor *Pitx2* and the *Chd7*

NIH-PA Author Manuscript

NIH-PA Author Manuscript

NIH-PA Author Manuscript

gene, which is associated with CHARGE syndrome (Nowotschin et al., 2006; Choi and Klingensmith, 2009; Randall et al., 2009).

The Sprouty genes encode intracellular regulators of RTK signaling and have been shown to function widely to regulate the levels and extent of signaling during embryonic development. Although signaling downstream of many growth factors can be regulated by Sprouty *in vitro*, *in vivo* evidence thus far seems to suggest a preference for the FGF and GDNF/RET pathways during mammalian development (Basson et al., 2005; Shim et al., 2005; Klein et al., 2006; Taniguchi et al., 2007). The human and mouse genomes contain four Sprouty genes, *Spry1-Spry4*. We found that two of these genes, *Spry1* and *Spry2* were co-expressed at high levels in all key tissues of the developing pharyngeal apparatus of the mouse embryo. We hypothesized that Sprouty genes play important roles in the development of the PA and that these genes may modify the phenotypes in mouse models of 22q11DS. Here we provide experimental evidence in support of this hypothesis, by showing that Sprouty-deficient embryos have many defects in organs derived from the PA and that these genes interact with *Tbx1* during development.

Results

Sprouty genes are expressed in the developing pharyngeal apparatus

Sprouty genes are feedback antagonists of FGF signalling and previous studies have reported Sprouty gene expression in the developing pharyngeal region of the mouse embryo where several FGF ligands are expressed (Minowada et al., 1999). We confirmed that *Spry1* and *Spry2* were expressed at high levels in the developing pharyngeal apparatus during the time when the anterior pharyngeal pouches are forming and the otic placode is invaginating to form the otic vesicle (Fig. 1A,B). We recently reported that these genes are expressed in the pharyngeal ectoderm, endoderm and mesoderm (Simrick et al., 2011). Sprouty gene expression is maintained in discrete regions in and around the anterior pharyngeal pouches after their formation and during the formation of the caudal pouches (Fig. 1D,E). As expected, Sprouty gene expression significantly overlapped with the expression of *Etv5* (*Erm*), another gene known to be transcriptionally regulated by FGF signaling (Klein et al., 2008) (Fig. 1C,F).

Spry1-/-;Spry2-/- (Spry1;2dko) embryos present with a range of pharyngeal phenotypes

Given the overlapping expression patterns of *Spry1* and *Spry2*, and the similar activities of SPRY1 and SPRY2 proteins on RTK signaling (Hanafusa et al., 2002; Iatan et al., 2009), we predicted that these genes would function redundantly in the pharyngeal apparatus. To directly test this hypothesis, we produced double *Spry1;Spry2* gene knockout embryos (*Spry1;2dko*) by crossing males homozygous for β*actin-Cre* and heterozygous for *Spry1* and *Spry2* null alleles (β*actin-Cre;Spry1+/-;Spry2+/-*) with females homozygous for conditional (flanked by loxP sites = flox) *Spry1* and *Spry2* alleles ($Spry1^{flox/flox};Spry2^{flox/flox}$) (Basson et al., 2005; Shim et al., 2005). β*actincre;Spry1+/- ;Spry2+/-* embryos (hereafter referred to as *Spry1+/-;Spry2+/-)* produced in these crosses were phenotypically normal and were used as littermate controls in all experiments.

NIH-PA Author Manuscript

NIH-PA Author Manuscript

NIH-PA Author Manuscript

Compound Sprouty gene knockout embryos were screened for the anomalies associated with 22q11DS. Velopharyngeal insufficiency due to cleft palate is a common birth defect associated with 22q11DS. Micro-MRI scanning of E15.5 embryos (Fig. 2) and direct examination of E16.5-E18.5 palates revealed severe clefting of the secondary palate in *Spry1;2dko* embryos (Fig. 2A, Table 1). Coronal sections through the heads of these embryos indicated that palatal shelves were present bilaterally, but that the shelves on at least one side of the embryo failed to elevate above the tongue (Fig. 2B). *Spry1+/-;Spry2-/-* (Fig. 2C,D) and *Spry1-/-;Spry2+/-* (Fig. 2E,F) embryos also presented with cleft palate, although these clefts were generally smaller, only affecting the posterior half of the palate (Fig. 2C,E). Interestingly, coronal sections through these embryos revealed palatal shelves that had elevated above the tongue, but failed to meet at the midline (Fig. 2D,F). *Spry1+/-;Spry2+/-* embryos (Fig. 2G,H) did not exhibit cleft palate. These data indicated that Sprouty genes controlled palatal development in a gene dosage-dependent manner. Furthermore, we noticed that the incidence of palatal defects did not increase gradually as Sprouty gene dosage was reduced, but that an apparent threshold was crossed between the loss of two and three Sprouty alleles, resulting in an increased incidence from 0% in *Spry1+/-;Spry2+/-* embryos to 100% in *Spry1+/-;Spry2-/-* and *Spry1-/-;Spry2+/-* embryos (Table 1).

Next we determined the position and size of the thymus, an organ often affected in DiGeorge syndrome. In *Spry1+/-;Spry2+/-* control embryos, the thymic lobes had descended completely to their final position at the mediastinum just cranially and ventrally to the heart by E15.5 (see Fig. 5B). The *Spry1;2dko* embryos had two thymus lobes, similar to controls, but thymi were hypoplastic and located ectopically in the neck of all mutant embryos analysed (Fig. 5C,D). Thymus abnormalities in *Spry1+/-;Spry2+/-* and all other embryos retaining at least one copy of *Spry1* or *Spry2* were generally mild and occurred at low frequencies (Table 2).

No defects in the outflow tract or major thoracic vessels were detected in *Spry1;2dko* embryos. However, 2/8 embryos had small ventricular septal defects (VSDs) (Table 3, data not shown).

In addition to the defects described here, we have also noted abnormalities in the parathyroids (JG, MAB and Nancy Manley, manuscript submitted). Thus, a range of phenotypes associated with 22q11del syndrome is present in embryos with reduced *Spry1* and *Spry2* gene dosage. These embryos may therefore represent useful mouse models for investigating the development of a subset of organs defective in this syndrome.

Pharyngeal arch artery defects in Spry1;2dko embryos

The pharyngeal arch arteries undergo a complex asymmetric remodeling process during development to form the large thoracic vessels, including the aortic arch. Aberrant loss or maintenance of segments of the embryonic PAAs is the primary cause of aortic arch defects (Srivastava and Olson, 2000; Hiruma et al., 2002). For example, the left-sided 4th PAA contributes to the portion of the descending aorta between the left common carotid (LCC) and left subclavian arteries (LSA). The absence of this portion of the aortic arch is referred to as interrupted aortic arch type B (IAA-B) and is a characteristic defect in 22q11del

NIH-PA Author Manuscript

NIH-PA Author Manuscript

NIH-PA Author Manuscript

syndrome . The pharyngeal arch arteries can be visualized at E10.5 of development by intracardiac India ink injections, which allowed us to determine the incidence of 4th PAA abnormalities. Wildtype and *Spry1+/-;Spry2+/-* embryos had normal pharyngeal arch arteries (Fig. 3A,B). A significant proportion (n=7/18) of *Spry1;2dko* embryos exhibited an abnormal regression of the 4th PAA at E10.5 (Fig. 3Eii, K). 4th PAA defects were also detected in embryos in which three Sprouty genes had been deleted: *Spry1-/-;Spry2+/-* and *Spry1+/-;Spry2-/-* (Fig. 3C-D, K, Table 3). Defects in other arch arteries were also observed. By E10.5 of development (35 somite stage), cranial arch arteries (1st and 2nd) had completely regressed in control embryos (Table 3). Similarly, no significant incidence of persistent 1st or 2nd arteries were observed in *Spry1-/-;Spry2+/-*, *Spry1+/-;Spry2-/-* embryos. *Spry1;2dko* embryos did not show a significant 1st PAA phenotype either (Table 3). However, persistent 2nd PAA defects occurred at high frequency in *Spry1;2dko* embryos (Fig. 3Ei, Table 3). Thus, *Spry1;2dko* embryos exhibited 2nd and 4th PAA defects at E10.5.

Sprouty genes interact with Tbx1 during PA development

Sprouty and *Tbx1* genes have been shown to regulate FGF signaling, albeit in apparently opposite ways, with *Tbx1* being required for FGF gene expression and Sprouty inhibiting FGF signal transduction. The apparent phenotypic similarities between Sprouty and *Tbx1* mutant embryos with respect to craniofacial, pharyngeal arch artery and thymus defects, suggested that Sprouty genes and *Tbx1* either affected the FGF (or another) pathway in a similar way, or that hypo- or hyperactivation of the pathway could result in similar phenotypes. We generated embryos with different allelic combinations of *Spry1*, *Spry2* and *Tbx1* loss of function alleles and determined their phenotypes in an attempt to distinguish between these possibilities. We reasoned that a phenotypic rescue would indicate that these mutations had opposing effects on signaling, whereas an exacerbation in the phenotype, would indicate that Sprouty and *Tbx1* mutation could affect the same pathway in a similar way.

Tbx1+/- embryos exhibit a low incidence of cardiovascular defects on certain genetic backgrounds (Merscher et al., 2001). The sensitivity of these defects to genetic background has also been reported in a mouse model in which the chromosomal region syntenic with the human critical region was deleted on one chromosome (Taddei et al., 2001). With the exception of one embryo (n=1/17), no cardiovascular defects were observed in *Tbx1+/-* mutants maintained on a mixed genetic background in our colony. This observation is in agreement with the low incidence of cardiovascular (9%) defects in these mutants reported previously (Liao et al., 2004). As all four *Spry1* and *Spry2* alleles had to be deleted before significant PAA defects were detected (Table 3), we chose to analyse embryos with various combinations of *Spry1*, *Spry2* and *Tbx1* null alleles.

To test for genetic interactions between Sprouty and *Tbx1* genes, we first visualised the PAAs in E10.5 embryos by ink injection. The incidence of 1st PAA persistence in *Tbx1+/-* or *Spry1;2dko* embryos was significantly increased when these mutations were combined in *Spry1;2dko;Tbx1+/-* embryos (Fig. 3J, Table 3). The incidence of 2nd and 4th PAA defects in *Spry1;2dko* embryos was also significantly increased on a *Tbx1+/-* background (Fig. 3, Table 3). First and second PAA defects are not normally observed in *Tbx1+/-* embryos.

NIH-PA Author Manuscript

NIH-PA Author Manuscript

NIH-PA Author Manuscript

Importantly, *Tbx1* heterozygosity also increased the incidence of 4th PAA defects significantly in *Spry1-/-;Spry2+/-*, *Spry1+/-;Spry2-/-* and even in *Spry1+/-;Spry2+/-* embryos (Fig. 3F-I, K, Table 3). These data indicate that Sprouty and *Tbx1* genes interacted during PAA development and that a reduction in gene dosage significantly increased the incidence of 4th PAA phenotypes. We concluded from these experiments that Sprouty and *Tbx1* loss of function mutations had similar effects on a genetic pathway that regulated PAA development.

To determine the consequences of these early PAA defects and to provide a more comprehensive picture of cardiovascular defects, we analysed E15.5-E17.5 embryos by micro-MRI, India ink injections and histology. The only cardiovascular defect observed in Sprouty-deficient embryos was ventricular septal defects that occurred at low frequency (e.g. n=2/8 in *Spry1;2dko* embryos, Table 3). Despite the clear PAA defects in many *Spry1;2dko* embryos at E10.5, no large thoracic vessel phenotypes were observed in Sprouty mutants at E15.5 (Fig. 4A,E,G,I and Table 3). A similar discrepancy between early pharyngeal arch artery and later aortic arch defects has been reported previously in *Tbx1+/-* mutants. Although defects in PAA development is associated with cardiovascular defects such as IAA-B, it has been shown that embryos with PAA defects at E10.5 appear to have the ability to repair/rescue a significant number of these early defects (Lindsay et al., 2001). These data indicated that Sprouty-deficient embryos could also recover from aortic arch defects after E10.5.

The increased severity of PAA defects at E10.5 in Sprouty;*Tbx1* compound mutants resulted in severe great vessel defects at E15.5 (Fig. 4, Table 3). The loss of three or four Sprouty alleles in combination with one *Tbx1* allele was associated with clear aortic arch defects at E15.5. The observed defects included retroesophageal aortic arch (Fig. 4C,H) and interrupted aortic arch type B (Fig. 4J). Both these defects are caused by the absence of a left 4th arch artery, resulting in an interruption between the left common carotid and left subclavian arteries. Embryos with vascular rings were also observed (Fig. 4D), a defect that can arise due to a persistant bilateral 4th aortic arch. The incidence of these defects was significantly increased compared to *Tbx1+/+* embryos of the corresponding Sprouty genotype (Table 3). Although a few *Spry1+/-;Spry2+/-;Tbx1+/-* embryos exhibited aortic arch defects (n=4/38), this low incidence was not statistically different from *Spry1+/-;Spry2+/-;Tbx1+/+* embryos. Mild outflow tract rotation defects were only observed in a small subset of *Spry1-/-;Spry2-/-;Tbx1+/-* embryos and not in any other genotype (Table 3). We concluded from this data that *Tbx1* haploinsufficiency significantly exacerbated PAA defects in Sprouty-deficient embryos and that the exacerbated phenotype at E10.5 correlated well with an increased incidence of great vessel anomalies by E15.5.

Sprouty and Tbx1 genes interact during thymus organogenesis

A small fraction (n=7/32) of *Tbx1+/-* embryos analysed had thymus hypoplasia (defined as <1/3 of the mean of control thymus size) (Fig. 5A, Table 2). A significant incidence of thymus defects was only observed upon the deletion of both Sprouty genes, and all these *Spry1;2dko* embryos exhibited thymus hypoplasia with thymus lobes located ectopically in the neck (Fig. 5D, Table 2). All of these embryos had two thymus lobes each, although only

NIH-PA Author Manuscript

NIH-PA Author Manuscript

NIH-PA Author Manuscript

one could be seen in many sections due to variability in their ectopic locations (Fig. 5C). By contrast, when *Tbx1* gene dosage was reduced in *Spry1;2dko* embryos, a significant number exhibited thymus aplasia (Fig. 5E,F, Table 2). *Tbx1* heterozygosity also had significant effects on thymus size in other Sprouty-deficient embryos. *Spry1+/-;Spry2-/-* embryos that had normal thymus development on a *Tbx1+/+* background, showed a significant increase in the incidence of thymus hypoplasia on a *Tbx1+/-* background (Table 2).

Sprouty genes interact with Tbx1 during palatogenesis

All embryos in which 3 or 4 Sprouty alleles had been deleted have cleft palate (Fig. 2, Table 1). *Tbx1* heterozygosity does not significantly alter the incidence of this phenotype (Table 1). No *Spry1+/-;Spry2+/-* or *Tbx1+/-* embryos with palatal defects were observed during the course of our study (Fig. 5G,H, Table 1). Intriguingly, many *Spry1+/-;Spry2+/-;Tbx1+/-* embryos had cleft palate, and the incidence of cleft palate in these mutants was significantly increased compared to *Spry1+/-;Spry2+/-* embryos (Fig. 5I,J, Table 1). Thus, it appears that *Tbx1* heterozygosity also sensitized the embryos to palatal defects.

Expanded Tbx1 expression in Spry1;2dko embryos

One possible explanation for the exacerbation of pharyngeal phenotypes by reducing *Tbx1* gene dosage in *Spry1;2dko* embryos, is that *Tbx1* gene expression may be downregulated in *Spry1;2dko* embryos. An examination of *Tbx1* expression in embryos between E9.0 and E9.5 revealed an expansion of *Tbx1* expression in the caudal (II-VI) arches (Fig. 6). The expansion of *Tbx1*-expressing core mesoderm in the second arch correlated with the increased size of this arch in these embryos, suggested that the expansion of Tbx1-expressing tissue is responsible for this phenotype (Simrick et al., 2011). This observation argued against a simple model whereby reduced *Tbx1* expression could account for the observed genetic interactions.

Tbx1 protects the embryos against mild perturbations in RTK signaling

As both TBX1 and Sprouty have been associated with the regulation of RTK signaling, in particular FGF signaling, we investigated to what extent the level of FGF signaling in the developing pharyngeal apparatus was perturbed in the various mutants. As all previous studies that concluded that TBX1 was an upstream, positive regulator of FGF signaling, only reported changes in FGF gene expression in *Tbx1* null embryos, we first wanted to determine whether FGF signaling was downregulated in *Tbx1+/-* embryos. As both *Spry1* (Basson et al., 2008) and *Spry2* (Chambers et al., 2000) genes are transcriptional read-outs of FGF signaling in the embryo, we monitored their expression in wildtype (*WT*), *Tbx1+/-* and *Tbx1-/-* embryos. Both *Spry1* (Fig. 7A-C, n=2/2) and *Spry2* (Fig. 7D-F, n=2/2) expression was downregulated in the pharyngeal apparatus of *Tbx1* mutant embryos in a manner that was clearly proportionate to the *Tbx1* gene dosage. Next, we compared the expression of another FGF read-out, *Etv5* (Klein et al., 2006). *Etv5* expression appeared slightly downregulated in *Tbx1+/-* mutants compared to wild type controls (Fig. 8A,B, n=4/4), perhaps clearest in the 1st pharyngeal arch (PA1). As expected, the expression levels of *Etv5* was increased in Sprouty mutant embryos, with the extent of upregulation correlating with the number of Sprouty alleles deleted: slight upregulation in

NIH-PA Author Manuscript

NIH-PA Author Manuscript

NIH-PA Author Manuscript

Spry1+/-;Spry2+/- (Fig. 8C) and stronger upregulation in *Spry1;2dko* embryos (Fig. 8E, n=4/4), consistent with these genes functioning as RTK antagonists. To our surprise, *Etv5* expression was drastically upregulated in many *Spry1+/-;Spry2+/-;Tbx1+/-* (Fig. 8D, n=2/3) and *Spry1;2dko;Tbx1+/-* (Fig 8F, n=2/4) embryos compared to stage-matched *Spry1+/-;Spry2+/-* and *Spry1;2dko* embryos. Quantitation of *Etv5* mRNA levels in microdissected pharyngeal tissue by quantitative RT-PCR, confirmed a significant upregulation of *Etv5* expression in *Spry1;2dko;Tbx1+/-* embryos compared to stage-matched *Spry1;2dko;Tbx1+/+* embryos (Fig. 8G). These observations suggest that the ability of *Tbx1* heterozygosity to enhance the phenotypes associated with Sprouty gene deficiency may be due to a significant upregulation of RTK signalling. To find further evidence for this, we also quantified the expression of several other genes that are transcriptionally regulated by RTK signaling. Both *Dusp6* and *Spry4* were upregulated in *Spry1;2dko;Tbx1+/-* embryos compared to *Spry1;2dko* embryos (Fig. 8G). We also measured *Fgfr1* transcript levels and found a slight, but significant increase, consistent with the observed increased RTK signaling. By contrast, *Fgf8* gene expression was not altered by the loss of one *Tbx1* allele, suggesting that increased *Fgf8* expression is unlikely to account for our observations (Fig. 8G).

Discussion

In the present study, we investigated the role of two Sprouty genes in pharyngeal development. Our data indicate that *Spry1* and *Spry2* function redundantly during PA development and that several functions are only revealed when more than one Sprouty gene is deleted, consistent with observations in other organs (Taniguchi et al., 2007; Klein et al., 2008). The most intriguing observation reported here is that *Tbx1* heterozygosity enhanced all these phenotypes, indicating that Sprouty and *Tbx1* genes functioned in the same or parallel genetic pathways and that loss of function Sprouty mutations should be considered as potential genetic modifiers of human phenotypes caused by *TBX1* haploinsufficiency.

TBX1 is a prime candidate for DiGeorge syndrome and the observation that *Tbx1* null mouse embryos exhibited severe defects in the formation of the caudal pharyngeal arches provided strong experimental evidence in support of the idea that *Tbx1* is a key player in pharyngeal apparatus development (Jerome and Papaioannou, 2001; Lindsay et al., 2001). Studies demonstrating that the expression of several genes encoding FGF ligands in the pharyngeal apparatus are lost in *Tbx1* null embryos placed TBX1 upstream of FGF signaling. Furthermore, *Fgf8* heterozygosity enhances the mild phenotypes present in *Tbx1+/-* embryos, in agreement with TBX1 being a positive regulator of FGF signaling (Vitelli et al., 2002; Aggarwal et al., 2006). The data presented in this manuscript argues against a simple linear model where TBX1 functions strictly as an upstream, positive regulator of FGF gene expression in all contexts. Indeed, a previous study reported that *Fgf8* overexpression in *Tbx1*-expressing cells that were also *Tbx1+/-*, enhanced the 4th PAA phenotypes (Vitelli et al., 2006). This observation is consistent with our findings. However, other phenotypes (e.g. thymus and palate) were not enhanced in this study and the authors concluded that the PAA phenotype was somehow unique with respect to FGF signalling. Our data now suggests that this phenomenon is applicable to other organs too and that the effect of TBX1 on FGF signalling thresholds may be more universal than previously thought.

NIH-PA Author Manuscript

NIH-PA Author Manuscript

NIH-PA Author Manuscript

A recent study in which the effects of reducing *Tbx1* transcript levels by small intervals were assessed, showed that the appearance of developmental defects did not correlate in a linear fashion with *Tbx1* levels, but rather that it exhibited an abrupt appearance of defects once *Tbx1* levels were reduced below a certain threshold. These results suggested that the maintenance of *Tbx1* levels within a certain range was required for the stability of the developmental system and that the sensitivity of an embryo to stochastic or environmental variation may be increased substantially when *Tbx1* levels approached this critical threshold. This interpretation is consistent with a model whereby both genetic and stochastic factors could contribute to the severity of the disease, as is indeed suggested by observations of discordant phenotypes in monozygotic twins (Goodship et al., 1995; Yamagishi et al., 1998; Vincent et al., 1999; Hillebrand et al., 2000), and the variation in phenotypic severity in inbred mouse strains (Jerome and Papaioannou, 2001; Taddei et al., 2001). TBX1 therefore appears to function as a central component that is required for the stability of the gene regulatory network(s) that control pharyngeal development (Baldini, 2005).

Our data appear to be in disagreement with two recent reports of cleft palate in *Spry2*-deficient mice on a C57BL/6J genetic background (Welsh et al., 2007; Matsumura et al., 2011). Mice homozygous for a targeted deletion of the *Spry2* open reading frame used in our experiments do not have cleft palate, even on a C57BL/6J background (Gail Martin, personal communication). The reason for this discrepancy is unknown, however, our studies indicate that Sprouty genes are required for normal palatal development, in a dosage-dependent manner.

Our data suggested that increasing RTK signaling by simultaneously deleting *Spry1* and *Spry2* resulted in phenotypes in many of the same organs typically affected by the loss or gain of *Tbx1* function (Funke et al., 2001; Merscher et al., 2001; Liao et al., 2004; Vitelli et al., 2009). The *Tbx1+/-* embryos used in the present study were generated from the $Tbx1^{tm1.2Bem}$ conditional allele (Arnold et al., 2006a). Most of these embryos appeared phenotypically normal on our mixed genetic background (129Sv;C57BL/6J; FVB/N; CD1), making it ideal to test for exacerbated phenotypes. The analyses of compound *Spry1;Spry2;Tbx1* mutants revealed a strong interaction between these mutations during PA development, suggesting that these genes functioned in the same or parallel genetic pathways.

To understand the reason for these genetic effects, we investigated whether RTK signaling was deregulated in unexpected ways in compound mutant embryos at a critical time point for caudal PA development (Xu et al., 2005). To our surprise, we found that the level of RTK signaling was disproportionally enhanced in Sprouty-deficient embryos on a *Tbx1+/-* background. We conclude that *Tbx1* heterozygosity “sensitized” the embryo to perturbations in FGF signaling. Thus, it appears that TBX1 has a crucial role in maintaining the stability of the developmental system and essentially functioned like a buffer against the perturbation of RTK signaling (Fig. 9).

The exact molecular mechanism whereby TBX1 might maintain the stability of the developmental system is not known. One possibility is that TBX1 does so by interacting with and integrating a large network of signaling pathways. *Tbx1* has indeed been shown to

NIH-PA Author Manuscript

NIH-PA Author Manuscript

NIH-PA Author Manuscript

interact with a number of major signaling pathways, including those regulated by FGF (Abu-Issa et al., 2002; Vitelli et al., 2002; Aggarwal et al., 2006), VEGF (Stalmans et al., 2003), Retinoic acid (Guris et al., 2006; Roberts et al., 2006), BMP (Fulcoli et al., 2009), SHH (Garg et al., 2001; Yamagishi et al., 2003), and Notch (Mitsiadis et al., 2010). The developing PA is a region in which all these signaling pathways are active and cells presumably integrate signals from this complex milieu. Thus, TBX1 may stabilise this system by functioning as an important integrator of many of these pathways. Although TBX1 may achieve this at the level of transcription, recent studies by the Baldini group have identified roles for TBX1 that appear distinct from its transcriptional activity. For example, TBX1 interacts with Serum Response Factor (SRF) and targets it for degradation (Chen et al., 2009) and interacts with SMAD1 to suppress BMP signaling (Fulcoli et al., 2009). Future studies are required to identify and characterize the individual interactions further, as well as integrate these interactions to understand the role of TBX1 at a “systems” level. Intriguingly, TBX1 has also been shown to be required for a mixed population of embryonic fibroblasts to respond to FGF8 in vitro, suggesting that TBX1 may have a more direct role in regulating FGF-responsiveness in cells (Herbst et al., 2010). Whether Sprouty and Tbx1 genes function in the same cell type e.g. the pharyngeal ectoderm to control neural crest migration will require the systematic analysis of mutants in which all these genes had been ablated in a cell type-specific manner (Eichenauer et al., 2009).

We found that different organs exhibited different sensitivities to alterations in RTK signaling and *Tbx1* levels. The most sensitive developmental system to Sprouty gene dosage appears to be the palate, with the arch arteries and thymus being relatively insensitive. Interestingly, we observed an extremely low incidence of heart (outflow tract and ventricular septum) defects in the Sprouty mutants and no significant genetic interaction with *Tbx1*. Zhang *et al.* also found that these structures were the least sensitive to the reduction in *Tbx1* transcript level (Zhang and Baldini, 2008). Vitelli et al. also found no exacerbation of outflow tract defects in *Tbx1*+/- embryos when overexpressing *Fgf8* (Vitelli et al., 2006). Two groups recently reported that the inhibition of FGF signaling in the secondary heart field by overexpressing *Spry1* or *Spry2* resulted in OFT defects (Park et al., 2008; Yang et al., 2010). Our data suggest that increased FGF signaling in the absence of *Spry1* and *Spry2* is still compatible with normal OFT development.

The observations reported here have important implications for our understanding of the aetiology underlying 22q11DS. One implication of our findings is that genetic, epigenetic or environmental factors that perturb RTK signaling during the critical time of development of the PA may have disproportionally large effects on *Tbx1*+/- embryos. Our data suggest that environmental insults enhance RTK signalling, in addition to those that can potentially reduce *Fgf8* expression, are likely to exacerbate phenotypes in *Tbx1*-deficient embryos (Vitelli et al., 2002; Sparrow et al., 2012). These interactions may account for the large clinical variability observed in 22q11DS patients.

NIH-PA Author Manuscript
NIH-PA Author Manuscript
NIH-PA Author Manuscript

Experimental Procedures

Mouse strains, breeding and genotyping

All mutant lines used in this study have been described previously and were maintained on a mixed genetic background; *βactin-cre* (Lewandoski et al., 1997), *Spry1* flox/null allele (Basson et al., 2005), *Spry2* flox/null allele (Shim et al., 2005) and *Tbx1 flox*/null allele (Arnold et al., 2006a). Mice homozygous for *β-actin cre* and heterozygous for *Spry1* and *Spry2* null alleles (β*cre*^{2}*;Spry1*+/-*;Spry2*+/-) were mated with mice homozygous for *Spry1* and *Spry2* flox alleles (Spry1$^{flox/flox}$;Spry2 $^{flox/flox}$). Sprouty;*Tbx1* compound mutants were generated either by mating β*cre*^{2}*;Spry1*+/-*;Spry2*+/-*;Tbx1*+/- mice with Spry1$^{flox/flox}$;Spry2 $^{flox/flox}$ mice, or by mating β*cre*^{2}*;Spry1*+/-*;Spry2*+/- mice with Spry1$^{flox/flox}$;Spry2$^{flox/flox}$*;Tbx1*$^{flox/flox}$ mice. Embryos were harvested from timed matings, where noon on the day of the vaginal plug was taken as E0.5. Harvested embryos were fixed overnight in 4% paraformaldehyde at 4°C, then either ink injected or dehydrated and stored in 100% methanol at -20°C for whole mount or section *in situ* hybridisation. E15.5 embryos collected for MRI scanning, were bled out into warm Hank's Balanced Salt solution before fixing in 4% formaldehyde at 4°C. In some cases, the chest cavities of E16.5-E18.5 embryos were opened and examined for the presence, position and size of thymus lobes and hearts removed for histological analysis. All experiments involving mice were approved by the BSU ethical review board, King's College London and were performed as specified by a UK Home Office Project Licence 70/9904.

Genotypes were determined by PCR amplification using embryonic yolk sac or tail DNA as appropriate. PCR primers for *βactin-cre* were CCT GGA AAA TGC TTC TGT CCG and CAG GGT GTT ATA AGC AAT CCC, which gave a 390bp product in cre positive embryos and no product in wild type embryos. *Spry1* genotyping primers were GGG AAA ACC GTG TTC TAA GGA GTA GC, GTT CTT TGT GGC AGA CAC TCT TCA TTC and CTC AAT AGG AGT GGA CTG TGA AAC TGC; which produced a 342bp product with a flox allele, a 150bp product with a null allele and a 311bp product with a wild type allele. Genotyping primers for *Spry2* were GGA TGG CTC TGA TCT GAT CC, TTG AGA ACA TGC CTC GAC C and GCA TGG GCT ATT CAC AAA C, resulting in PCR products of 500bp with a flox allele, a 225bp product with a null allele and a 350bp product with a wild type allele. *Tbx1* genotyping primers were TGA CTG TGC TGA AGT GCA TC, TCT TCT TGG GGC TGT AGA CT and AGC GCA ATG GCT TTT AAG GG, which generated a 580bp product with a flox allele, a 415bp product with a null allele and a 532 product with a wild type allele.

India ink injections

The pharyngeal arch arteries and the great arteries were visualized by Indian ink (Pelikan) injections into the outflow tract with a glass microinjection needle.

MRI

E15.5 embryos were dissected, exsanguinated and fixed in 4% PFA with Gd-DTPA for at least three days. Fixed embryos were embedded in agarose, also containing Gd-DTPA and MRI was performed as previously described in Schneider *et al.* (Schneider and

NIH-PA Author Manuscript

NIH-PA Author Manuscript

NIH-PA Author Manuscript

Bhattacharya, 2004). The analysis and 3D reconstructions of MRI data were done using the Amira® software (Visage Imaging Inc.).

Histology

Embryos were embedded in paraffin and sectioned at 7μm thickness in preparation for section immunohistochemistry or H&E staining. H&E (hematoxylin and eosin) staining was performed by Dr. Alasdair Edgar according to standard protocols.

In situ hybridisation

Whole mount RNA *in situ* hybridisation was performed according to standard protocols. *Spry1* and *Spry2* RNA probes were produced from constructs as described by Minowada *et al.* (Minowada et al., 1999). The *Etv5* (*Erm*) RNA probe has previously been detailed by Klein *et al.* (Klein et al., 2006).

Quantitative RT-PCR

The pharyngeal apparatus from stage-matched embryos (21-23ss) was microdissected and all adjacent neural and heart tube tissues removed. Total RNA was extracted and genomic DNA removed using the Absolutely RNA Microprep Kit (Agilent Technologies) . A total of 200ng of RNA was used for first-strand DNA synthesis with nanoScript Precision RT kit (PrimerDesign Ltd.) according to the manufacturer's specifications. cDNA synthesis reactions without reverse transcriptase enzyme (no RT) were used as controls for q-RT-PCR. qRT-PCR was performed on a RotorGene Q cycler (Qiagen) using Precision qPCR MasterMix kit (PrimerDesign Ltd.). Appropriate normalising genes were detected using qbasePLUS software (Biogazelle) with geNorm reference kits (PrimerDesign Ltd.) All reactions were performed twice in duplicate each time and normalised to GAPDH. Cq threshold values were determined manually and all were at least 5 Cq values below no RT controls. ΔΔCq values were calculated relative to *S12dko* samples using Microsoft Excel software and graphs were produced using GraphPad Prism software. Primers were as follows: *Etv5* (5’-TGCCCACTTCATCGCCTGGAC-3’ and 5’-TAGCGGAGAGAGCGGCTCAG-3’), Dusp6 (5’- TCTGTTTGAGAATGCGGGCGAG-3’ and 5’- GCCAAGCAATGCACCAGGACAC-3’), Spry4 (5’-TGCGACTTCAACGGCGACTG-3’ and 5’- ACTGCACCAAGGGACAGGCTTC-3’), Fgfr1 (5’- GGCAGCGATACCACCTACTTCTCC-3’ and 5’-GGCCTACGGTTTGGTTTGGTGTTG-3’), Fgf8 (5’-AGGTCTCTACATCTGCATGAAC-3’ and 5’- TGTTCTCCAGCACGATCTCT-3’), Tbx1 (5’- CGACAAGCTGAACTGACCA-3’ and 5’- CAATCTTAAGCTGCGTGATCC-3’) and *Gapdh* as a normaliser (F, 5’-AGGTCGGTGTGAACGGATTTG– 3’ and R, 5’-TGTAGACCATGTAGTTGAGGTCA-3’).

Supplementary Material

Refer to Web version on PubMed Central for supplementary material.

NIH-PA Author Manuscript

NIH-PA Author Manuscript

NIH-PA Author Manuscript

Acknowledgments

We thank Gail Martin in whose laboratory this project was initiated, for her support and for providing *βactin-cre* and *Spry2*^{flox} mouse lines, Gail Martin (*Spry1*, *Spry2*), Silvia Arber (*Etv5*) and Virginia Papaioannou (*Tbx1*) for generously provided *in situ* probes, Hagen Schmidt and Samantha Martin for technical assistance, Raj Thakker, Pete Scambler, Denny Monks and our laboratory colleagues for suggestions, discussions and comments on the manuscript. All animal experiments were approved by and performed according to a Project Licence from the UK Home Office. This work was supported by a grant from the Medical Research Council (G0601104) to MAB, a British Heart Foundation Chair Award (CH/09/003), EU FP7-HEALTH B Program Grant (223463) and Cardiogenet BHF Program Grant (RG/10/17/28553) to SB, and NIH grants (R01 HL088698 and P01 HD070454) to BM.

References

Abu-Issa R, Smyth G, Smoak I, Yamamura K, Meyers EN. Fgf8 is required for pharyngeal arch and cardiovascular development in the mouse. Development. 2002; 129:4613–4625. [PubMed: 12223417]

Aggarwal VS, Liao J, Bondarev A, Schimmang T, Lewandoski M, Locker J, Shanske A, Campione M, Morrow BE. Dissection of Tbx1 and Fgf interactions in mouse models of 22q11DS suggests functional redundancy. Hum Mol Genet. 2006; 15:3219–3228. [PubMed: 17000704]

Arnold JS, Braunstein EM, Ohyama T, Groves AK, Adams JC, Brown MC, Morrow BE. Tissue-specific roles of Tbx1 in the development of the outer, middle and inner ear, defective in 22q11DS patients. Hum Mol Genet. 2006a; 15:1629–1639. [PubMed: 16600992]

Arnold JS, Werling U, Braunstein EM, Liao J, Nowotschin S, Edelmann W, Hebert JM, Morrow BE. Inactivation of Tbx1 in the pharyngeal endoderm results in 22q11DS malformations. Development. 2006b; 133:977–987. [PubMed: 16452092]

Baldini A. Dissecting contiguous gene defects: TBX1. Curr Opin Genet Dev. 2005; 15:279–284. [PubMed: 15917203]

Basson MA, Akbulut S, Watson-Johnson J, Simon R, Carroll TJ, Shakya R, Gross I, Martin GR, Lufkin T, McMahon AP, Wilson PD, Costantini FD, Mason IJ, Licht JD. Sprouty1 is a critical regulator of GDNF/RET-mediated kidney induction. Dev Cell. 2005; 8:229–239. [PubMed: 15691764]

Basson MA, Echevarria D, Ahn CP, Sudarov A, Joyner AL, Mason IJ, Martinez S, Martin GR. Specific regions within the embryonic midbrain and cerebellum require different levels of FGF signaling during development. Development. 2008; 135:889–898. [PubMed: 18216176]

Botto LD, May K, Fernhoff PM, Correa A, Coleman K, Rasmussen SA, Merritt RK, O'Leary LA, Wong LY, Elixson EM, Mahle WT, Campbell RM. A population-based study of the 22q11.2 deletion: phenotype, incidence, and contribution to major birth defects in the population. Pediatrics. 2003; 112:101–107. [PubMed: 12837874]

Brown CB, Wenning JM, Lu MM, Epstein DJ, Meyers EN, Epstein JA. Cre-mediated excision of Fgf8 in the Tbx1 expression domain reveals a critical role for Fgf8 in cardiovascular development in the mouse. Dev Biol. 2004; 267:190–202. [PubMed: 14975726]

Carlson C, Papolos D, Pandita RK, Faedda GL, Veit S, Goldberg R, Shprintzen R, Kucherlapati R, Morrow B. Molecular analysis of velo-cardio-facial syndrome patients with psychiatric disorders. Am J Hum Genet. 1997; 60:851–859. [PubMed: 9106531]

Chambers D, Medhurst AD, Walsh FS, Price J, Mason I. Differential display of genes expressed at the midbrain - hindbrain junction identifies sprouty2: an FGF8-inducible member of a family of intracellular FGF antagonists. Mol Cell Neurosci. 2000; 15:22–35. [PubMed: 10662503]

Chen L, Fulcoli FG, Tang S, Baldini A. Tbx1 regulates proliferation and differentiation of multipotent heart progenitors. Circ Res. 2009; 105:842–851. [PubMed: 19745164]

Choi M, Klingensmith J. Chordin is a modifier of tbx1 for the craniofacial malformations of 22q11 deletion syndrome phenotypes in mouse. PLoS Genet. 2009; 5:e1000395. [PubMed: 19247433]

Driscoll DA, Boland T, Emanuel BS, Kirschner RE, LaRossa D, Manson J, McDonald-McGinn D, Randall P, Solot C, Zackai E, Mitchell LE. Evaluation of potential modifiers of the palatal phenotype in the 22q11.2 deletion syndrome. Cleft Palate Craniofac J. 2006; 43:435–441. [PubMed: 16854201]

NIH-PA Author Manuscript

NIH-PA Author Manuscript

NIH-PA Author Manuscript

Eichenauer DA, Bredenfeld H, Haverkamp H, Muller H, Franklin J, Fuchs M, Borchmann P, Muller-Hermelink HK, Eich HT, Muller RP, Diehl V, Engert A. Hodgkin's lymphoma in adolescents treated with adult protocols: a report from the German Hodgkin study group. J Clin Oncol. 2009; 27:6079–6085. [PubMed: 19901121]

Frank DU, Fotheringham LK, Brewer JA, Muglia LJ, Tristani-Firouzi M, Capecchi MR, Moon AM. An Fgf8 mouse mutant phenocopies human 22q11 deletion syndrome. Development. 2002; 129:4591–4603. [PubMed: 12223415]

Fulcoli FG, Huynh T, Scambler PJ, Baldini A. Tbx1 regulates the BMP-Smad1 pathway in a transcription independent manner. PLoS One. 2009; 4:e6049. [PubMed: 19557177]

Funke B, Epstein JA, Kochilas LK, Lu MM, Pandita RK, Liao J, Bauerndistel R, Schuler T, Schorle H, Brown MC, Adams J, Morrow BE. Mice overexpressing genes from the 22q11 region deleted in velo-cardio-facial syndrome/DiGeorge syndrome have middle and inner ear defects. Hum Mol Genet. 2001; 10:2549–2556. [PubMed: 11709542]

Garg V, Yamagishi C, Hu T, Kathiriya IS, Yamagishi H, Srivastava D. Tbx1, a DiGeorge syndrome candidate gene, is regulated by sonic hedgehog during pharyngeal arch development. Dev Biol. 2001; 235:62–73. [PubMed: 11412027]

Goldmuntz E, Driscoll DA, Emanuel BS, McDonald-McGinn D, Mei M, Zackai E, Mitchell LE. Evaluation of potential modifiers of the cardiac phenotype in the 22q11.2 deletion syndrome. Birth Defects Res A Clin Mol Teratol. 2009; 85:125–129. [PubMed: 18770859]

Gong W, Gottlieb S, Collins J, Blescia A, Dietz H, Goldmuntz E, McDonald-McGinn DM, Zackai EH, Emanuel BS, Driscoll DA, Budarf ML. Mutation analysis of TBX1 in non-deleted patients with features of DGS/VCFS or isolated cardiovascular defects. J Med Genet. 2001; 38:E45. [PubMed: 11748311]

Goodship J, Cross I, Scambler P, Burn J. Monozygotic twins with chromosome 22q11 deletion and discordant phenotype. J Med Genet. 1995; 32:746–748. [PubMed: 8544199]

Guris DL, Duester G, Papaioannou VE, Imamoto A. Dose-dependent interaction of Tbx1 and Crkl and locally aberrant RA signaling in a model of del22q11 syndrome. Dev Cell. 2006; 10:81–92. [PubMed: 16399080]

Hanafusa H, Torii S, Yasunaga T, Nishida E. Sprouty1 and Sprouty2 provide a control mechanism for the Ras/MAPK signalling pathway. Nat Cell Biol. 2002; 4:850–858. [PubMed: 12402043]

Herbst C, Rehan FA, Brillant C, Bohlius J, Skoetz N, Schulz H, Monsef I, Specht L, Engert A. Combined modality treatment improves tumor control and overall survival in patients with early stage Hodgkin's lymphoma: a systematic review. Haematologica. 2010; 95:494–500. [PubMed: 19951972]

Hillebrand G, Siebert R, Simeoni E, Santer R. DiGeorge syndrome with discordant phenotype in monozygotic twins. J Med Genet. 2000; 37:E23. [PubMed: 10978370]

Hiruma T, Nakajima Y, Nakamura H. Development of pharyngeal arch arteries in early mouse embryo. J Anat. 2002; 201:15–29. [PubMed: 12171473]

Iatan I, Dastani Z, Do R, Weissglas-Volkov D, Ruel I, Lee JC, Huertas-Vazquez A, Taskinen MR, Prat A, Seidah NG, Pajukanta P, Engert JC, Genest J. Genetic variation at the proprotein convertase subtilisin/kexin type 5 gene modulates high-density lipoprotein cholesterol levels. Circ Cardiovasc Genet. 2009; 2:467–475. [PubMed: 20031622]

Jerome LA, Papaioannou VE. DiGeorge syndrome phenotype in mice mutant for the T-box gene, Tbx1. Nat Genet. 2001; 27:286–291. [PubMed: 11242110]

Klein OD, Lyons DB, Balooch G, Marshall GW, Basson MA, Peterka M, Boran T, Peterkova R, Martin GR. An FGF signaling loop sustains the generation of differentiated progeny from stem cells in mouse incisors. Development. 2008; 135:377–385. [PubMed: 18077585]

Klein OD, Minowada G, Peterkova R, Kangas A, Yu BD, Lesot H, Peterka M, Jernvall J, Martin GR. Sprouty genes control diastema tooth development via bidirectional antagonism of epithelial-mesenchymal FGF signaling. Dev Cell. 2006; 11:181–190. [PubMed: 16890158]

Kobrynski LJ, Sullivan KE. Velocardiofacial syndrome, DiGeorge syndrome: the chromosome 22q11.2 deletion syndromes. Lancet. 2007; 370:1443–1452. [PubMed: 17950858]

Lewandoski M, Meyers EN, Martin GR. Analysis of Fgf8 gene function in vertebrate development. Cold Spring Harb Symp Quant Biol. 1997; 62:159–168. [PubMed: 9598348]

NIH-PA Author Manuscript

NIH-PA Author Manuscript

NIH-PA Author Manuscript

Liao J, Kochilas L, Nowotschin S, Arnold JS, Aggarwal VS, Epstein JA, Brown MC, Adams J, Morrow BE. Full spectrum of malformations in velo-cardio-facial syndrome/DiGeorge syndrome mouse models by altering Tbx1 dosage. Hum Mol Genet. 2004; 13:1577–1585. [PubMed: 15190012]

Lindsay EA, Vitelli F, Su H, Morishima M, Huynh T, Pramparo T, Jurecic V, Ogunrinu G, Sutherland HF, Scambler PJ, Bradley A, Baldini A. Tbx1 haploinsufficieny in the DiGeorge syndrome region causes aortic arch defects in mice. Nature. 2001; 410:97–101. [PubMed: 11242049]

Matsumura K, Taketomi T, Yoshizaki K, Arai S, Sanui T, Yoshiga D, Yoshimura A, Nakamura S. Sprouty2 controls proliferation of palate mesenchymal cells via fibroblast growth factor signaling. Biochem Biophys Res Commun. 2011; 404:1076–1082. [PubMed: 21195053]

McDermid HE, Morrow BE. Genomic disorders on 22q11. Am J Hum Genet. 2002; 70:1077–1088. [PubMed: 11925570]

Merscher S, Funke B, Epstein JA, Heyer J, Puech A, Lu MM, Xavier RJ, Demay MB, Russell RG, Factor S, Tokooya K, Jore BS, Lopez M, Pandita RK, Lia M, Carrion D, Xu H, Schorle H, Kobler JB, Scambler P, Wynshaw-Boris A, Skoultchi AI, Morrow BE, Kucherlapati R. TBX1 is responsible for cardiovascular defects in velo-cardio-facial/DiGeorge syndrome. Cell. 2001; 104:619–629. [PubMed: 11239417]

Minowada G, Jarvis LA, Chi CL, Neubuser A, Sun X, Hacohen N, Krasnow MA, Martin GR. Vertebrate Sprouty genes are induced by FGF signaling and can cause chondrodysplasia when overexpressed. Development. 1999; 126:4465–4475. [PubMed: 10498682]

Mitsiadis TA, Graf D, Luder H, Gridley T, Bluteau G. BMPs and FGFs target Notch signalling via jagged 2 to regulate tooth morphogenesis and cytodifferentiation. Development. 2010

Morrow B, Goldberg R, Carlson C, Das Gupta R, Sirotkin H, Collins J, Dunham I, O'Donnell H, Scambler P, Shprintzen R, et al. Molecular definition of the 22q11 deletions in velo-cardio-facial syndrome. Am J Hum Genet. 1995; 56:1391–1403. [PubMed: 7762562]

Nowotschin S, Liao J, Gage PJ, Epstein JA, Campione M, Morrow BE. Tbx1 affects asymmetric cardiac morphogenesis by regulating Pitx2 in the secondary heart field. Development. 2006; 133:1565–1573. [PubMed: 16556915]

Park EJ, Ogden LA, Talbot A, Evans S, Cai CL, Black BL, Frank DU, Moon AM. Required, tissue-specific roles for Fgf8 in outflow tract formation and remodeling. Development. 2006; 133:2419–2433. [PubMed: 16720879]

Park EJ, Watanabe Y, Smyth G, Miyagawa-Tomita S, Meyers E, Klingensmith J, Camenisch T, Buckingham M, Moon AM. An FGF autocrine loop initiated in second heart field mesoderm regulates morphogenesis at the arterial pole of the heart. Development. 2008; 135:3599–3610. [PubMed: 18832392]

Randall V, McCue K, Roberts C, Kyriakopoulou V, Beddow S, Barrett AN, Vitelli F, Prescott K, Shaw-Smith C, Devriendt K, Bosman E, Steffes G, Steel KP, Simrick S, Basson MA, Illingworth E, Scambler PJ. Great vessel development requires biallelic expression of Chd7 and Tbx1 in pharyngeal ectoderm in mice. J Clin Invest. 2009; 119:3301–3310. [PubMed: 19855134]

Roberts C, Ivins S, Cook AC, Baldini A, Scambler PJ. Cyp26 genes a1, b1 and c1 are down-regulated in Tbx1 null mice and inhibition of Cyp26 enzyme function produces a phenocopy of DiGeorge Syndrome in the chick. Hum Mol Genet. 2006; 15:3394–3410. [PubMed: 17047027]

Scambler PJ. The 22q11 deletion syndromes. Hum Mol Genet. 2000; 9:2421–2426. [PubMed: 11005797]

Scambler PJ, Carey AH, Wyse RK, Roach S, Dumanski JP, Nordenskjold M, Williamson R. Microdeletions within 22q11 associated with sporadic and familial DiGeorge syndrome. Genomics. 1991; 10:201–206. [PubMed: 2045103]

Schneider JE, Bhattacharya S. Making the mouse embryo transparent: identifying developmental malformations using magnetic resonance imaging. Birth Defects Res C Embryo Today. 2004; 72:241–249. [PubMed: 15495185]

Shim K, Minowada G, Coling DE, Martin GR. Sprouty2, a mouse deafness gene, regulates cell fate decisions in the auditory sensory epithelium by antagonizing FGF signaling. Dev Cell. 2005; 8:553–564. [PubMed: 15809037]

NIH-PA Author Manuscript

NIH-PA Author Manuscript

NIH-PA Author Manuscript

Simrick S, Lickert H, Basson MA. Sprouty genes are essential for the normal development of epibranchial ganglia in the mouse embryo. Dev Biol. 2011; 358:147–155. [PubMed: 21806979]

Sparrow DB, Chapman G, Smith AJ, Mattar MZ, Major JA, O'Reilly VC, Saga Y, Zackai EH, Dormans JP, Alman BA, McGregor L, Kageyama R, Kusumi K, Dunwoodie SL. A mechanism for gene-environment interaction in the etiology of congenital scoliosis. Cell. 2012; 149:295–306. [PubMed: 22484060]

Srivastava D, Olson EN. A genetic blueprint for cardiac development. Nature. 2000; 407:221–226. [PubMed: 11001064]

Stalmans I, Lambrechts D, De Smet F, Jansen S, Wang J, Maity S, Kneer P, von der Ohe M, Swillen A, Maes C, Gewillig M, Molin DG, Hellings P, Boetel T, Haardt M, Compernolle V, Dewerchin M, Plaisance S, Vlietinck R, Emanuel B, Gittenberger-de Groot AC, Scambler P, Morrow B, Driscol DA, Moons L, Esguerra CV, Carmeliet G, Behn-Krappa A, Devriendt K, Collen D, Conway SJ, Carmeliet P. VEGF: a modifier of the del22q11 (DiGeorge) syndrome? Nat Med. 2003; 9:173–182. [PubMed: 12539040]

Taddei I, Morishima M, Huynh T, Lindsay EA. Genetic factors are major determinants of phenotypic variability in a mouse model of the DiGeorge/del22q11 syndromes. Proc Natl Acad Sci U S A. 2001; 98:11428–11431. [PubMed: 11562466]

Taniguchi K, Ayada T, Ichiyama K, Kohno R, Yonemitsu Y, Minami Y, Kikuchi A, Maehara Y, Yoshimura A. Sprouty2 and Sprouty4 are essential for embryonic morphogenesis and regulation of FGF signaling. Biochem Biophys Res Commun. 2007; 352:896–902. [PubMed: 17156747]

Vincent MC, Heitz F, Tricoire J, Bourrouillou G, Kuhlein E, Rolland M, Calvas P. 22q11 deletion in DGS/VCFS monozygotic twins with discordant phenotypes. Genet Couns. 1999; 10:43–49. [PubMed: 10191428]

Vitelli F, Huynh T, Baldini A. Gain of function of Tbx1 affects pharyngeal and heart development in the mouse. Genesis. 2009; 47:188–195. [PubMed: 19253341]

Vitelli F, Taddei I, Morishima M, Meyers EN, Lindsay EA, Baldini A. A genetic link between Tbx1 and fibroblast growth factor signaling. Development. 2002; 129:4605–4611. [PubMed: 12223416]

Vitelli F, Zhang Z, Huynh T, Sobotka A, Mupo A, Baldini A. Fgf8 expression in the Tbx1 domain causes skeletal abnormalities and modifies the aortic arch but not the outflow tract phenotype of Tbx1 mutants. Dev Biol. 2006; 295:559–570. [PubMed: 16696966]

Welsh IC, Hagge-Greenberg A, O'Brien TP. A dosage-dependent role for Spry2 in growth and patterning during palate development. Mech Dev. 2007; 124:746–761. [PubMed: 17693063]

Wurdak H, Ittner LM, Sommer L. DiGeorge syndrome and pharyngeal apparatus development. Bioessays. 2006; 28:1078–1086. [PubMed: 17041894]

Xu H, Cerrato F, Baldini A. Timed mutation and cell-fate mapping reveal reiterated roles of Tbx1 during embryogenesis, and a crucial function during segmentation of the pharyngeal system via regulation of endoderm expansion. Development. 2005; 132:4387–4395. [PubMed: 16141220]

Yagi H, Furutani Y, Hamada H, Sasaki T, Asakawa S, Minoshima S, Ichida F, Joo K, Kimura M, Imamura S, Kamatani N, Momma K, Takao A, Nakazawa M, Shimizu N, Matsuoka R. Role of TBX1 in human del22q11.2 syndrome. Lancet. 2003; 362:1366–1373. [PubMed: 14585638]

Yamagishi H, Ishii C, Maeda J, Kojima Y, Matsuoka R, Kimura M, Takao A, Momma K, Matsuo N. Phenotypic discordance in monozygotic twins with 22q11.2 deletion. Am J Med Genet. 1998; 78:319–321. [PubMed: 9714432]

Yamagishi H, Maeda J, Hu T, McAnally J, Conway SJ, Kume T, Meyers EN, Yamagishi C, Srivastava D. Tbx1 is regulated by tissue-specific forkhead proteins through a common Sonic hedgehog-responsive enhancer. Genes Dev. 2003; 17:269–281. [PubMed: 12533514]

Yang X, Kilgallen S, Andreeva V, Spicer DB, Pinz I, Friesel R. Conditional expression of Spry1 in neural crest causes craniofacial and cardiac defects. BMC Dev Biol. 2010; 10:48. [PubMed: 20459789]

Zhang Z, Baldini A. In vivo response to high-resolution variation of Tbx1 mRNA dosage. Hum Mol Genet. 2008; 17:150–157. [PubMed: 17916582]

Zweier C, Sticht H, Aydin-Yaylagul I, Campbell CE, Rauch A. Human TBX1 missense mutations cause gain of function resulting in the same phenotype as 22q11.2 deletions. Am J Hum Genet. 2007; 80:510–517. [PubMed: 17273972]

NIH-PA Author Manuscript

NIH-PA Author Manuscript

NIH-PA Author Manuscript

Key findings

- Sprouty gene deletion results in multiple developmental phenotypes characteristic of 22q11.2 deletion syndrome
- Contrary to expectations, reducing the *Tbx1* gene dosage significantly exacerbates these phenotypes
- *Tbx1* haploinsufficiency in the context of Sprouty gene deletion is associated with increased Receptor Tyrosine Kinase (RTK) signalling, suggesting that TBX1 can prevent excessive RTK signalling levels during development

NIH-PA Author Manuscript
NIH-PA Author Manuscript
NIH-PA Author Manuscript

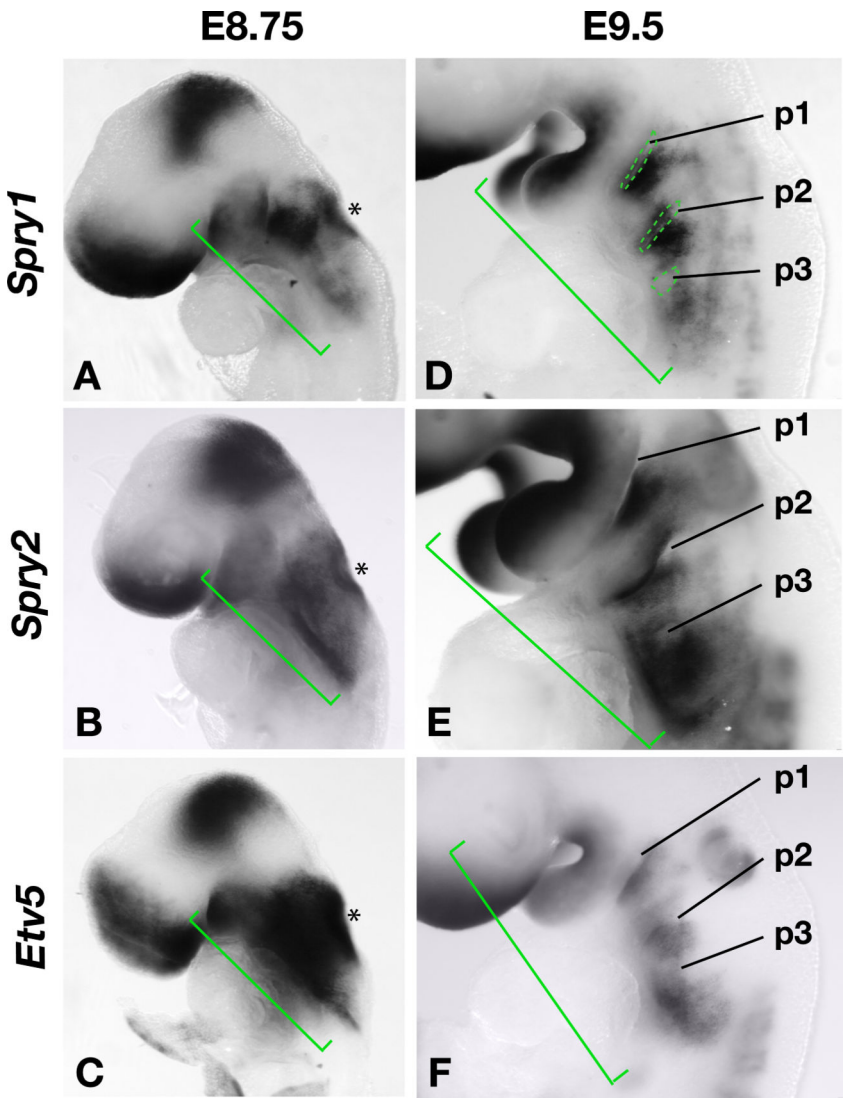

Figure 1. Sprouty and Etv5 gene expression in the developing pharyngeal apparatus of mouse embryos.

A-C) *Spry1*, *Spry2* and *Etv5* gene expression in the developing pharyngeal region (green brackets) and otic vesicle (asterisk) of mouse embryos at E8.75.

D-F) Gene expression in E9.5 embryos with the pharyngeal pouches (p1-p3) indicated.

NIH-PA Author Manuscript
NIH-PA Author Manuscript
NIH-PA Author Manuscript

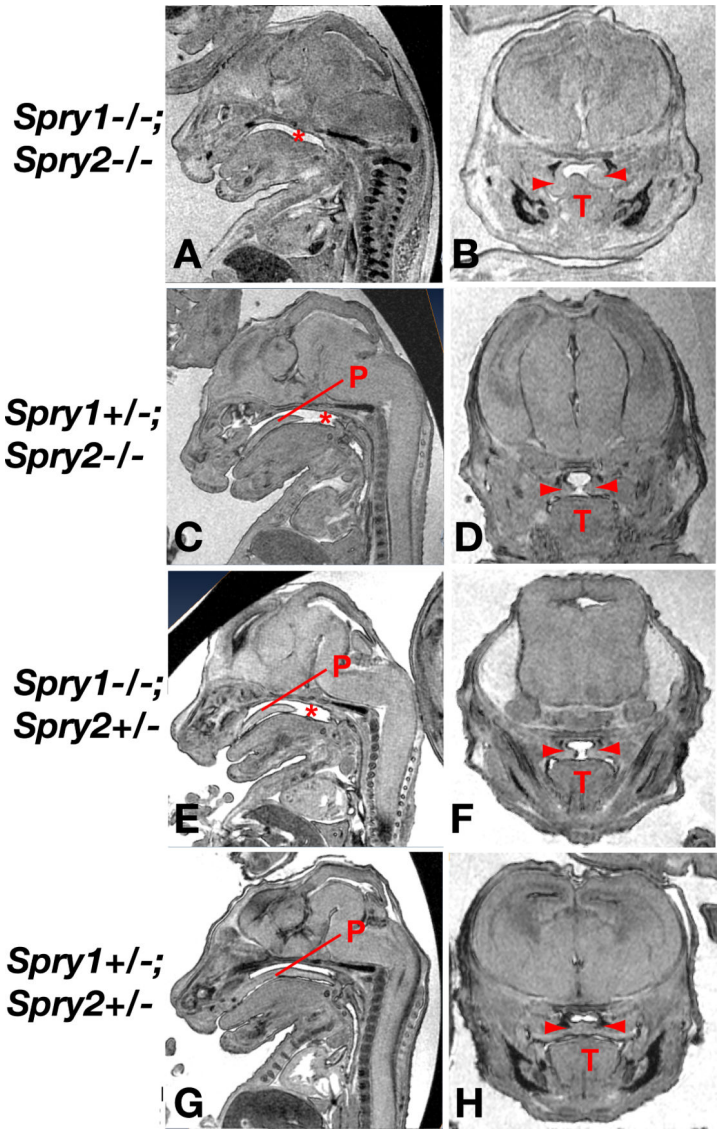

Figure 2. Palatal development is sensitive to Sprouty gene dosage

MRI sections of mutant E15.5 embryos in sagittal (A,C,E,G) or coronal (B,D,F,H) views. The absence of palatal tissue (P) is indicated by an asterisk and the two palatal shelves by red arrowheads. T=tongue.

NIH-PA Author Manuscript

NIH-PA Author Manuscript

NIH-PA Author Manuscript

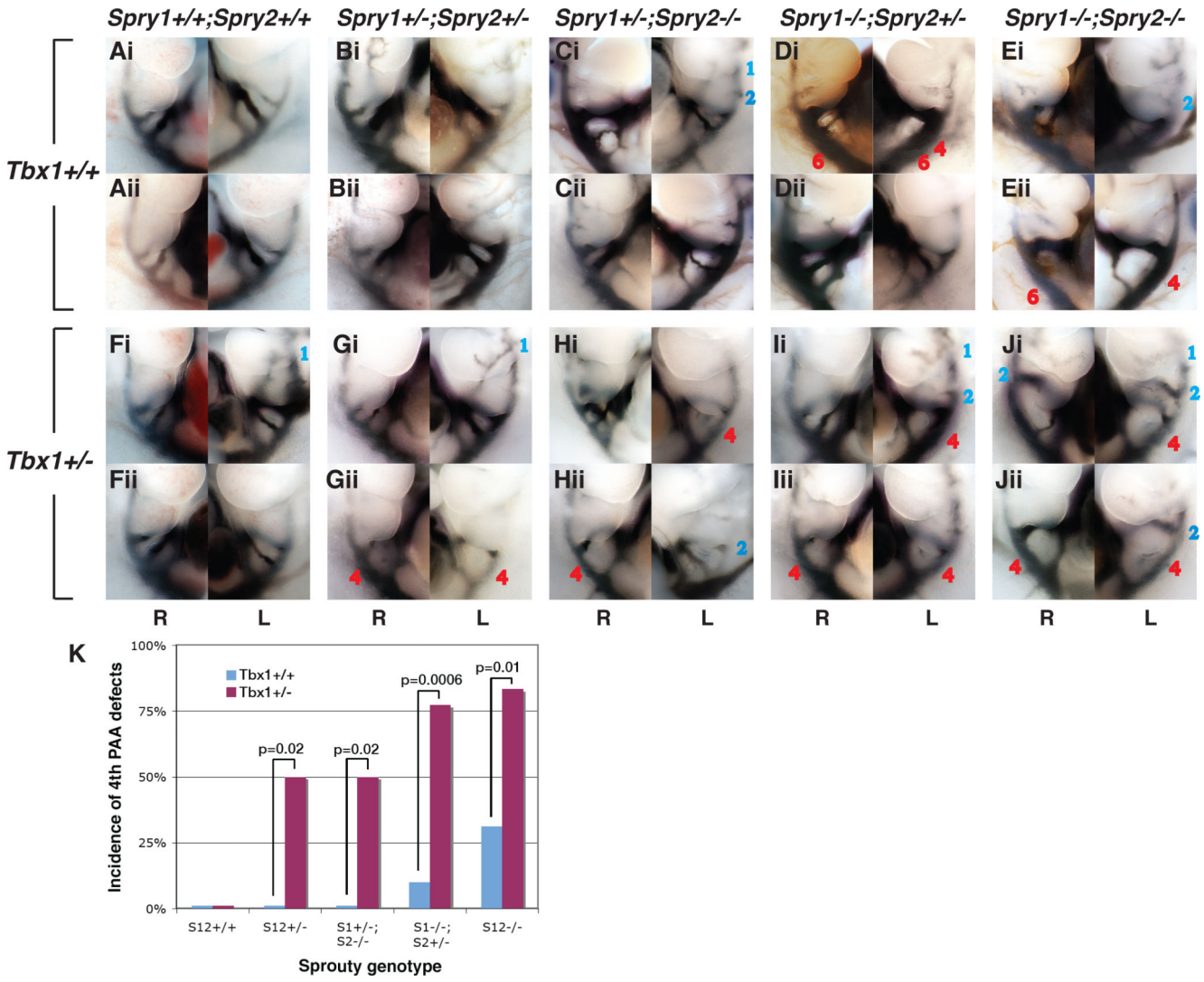

Figure 3. Examples of pharyngeal arch artery defects in Sprouty-deficient embryos on Tbx1 wildtype or heterozygous backgrounds

Micrographs of right (R) and left (L) sided views of E10.5 embryos with ink-filled aortic arch arteries are depicted. Examples of embryos with wildtype complement (A,F) or loss of 2-4 Spouty alleles (B-E, G-J) on a *Tbx1* wildtype (A-E) or *Tbx1*+/- (F-J) background are shown, two for each genotype (i and ii). Persistant arch arteries are labeled in blue and missing arteries in red.

K) The incidence of 4th PAA defects are indicated for each genotype, note the significant increase in incidence of this phenotype on a *Tbx1*+/- background for all four Sprouty-deficient genotypes.

NIH-PA Author Manuscript
NIH-PA Author Manuscript
NIH-PA Author Manuscript

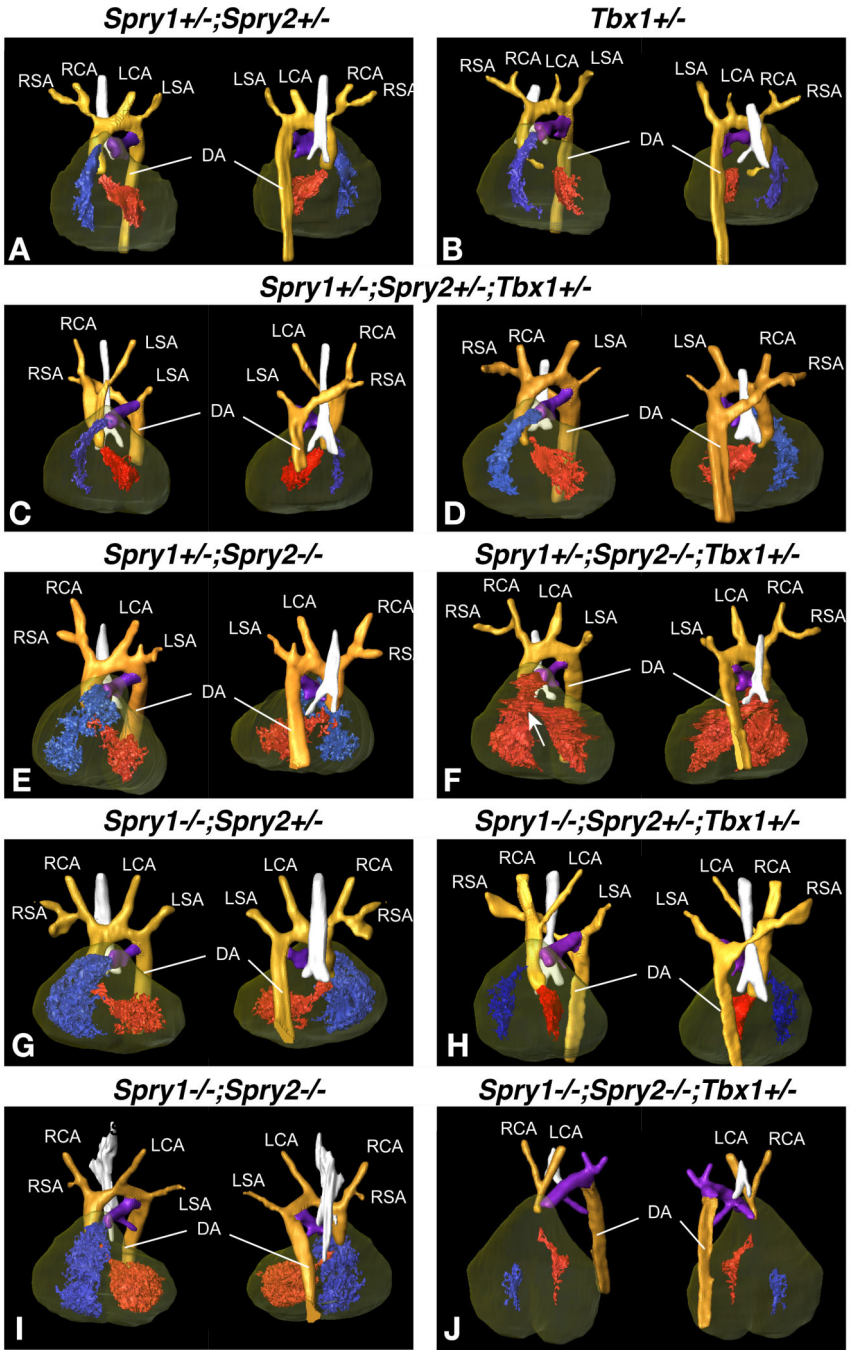

Figure 4. Anatomy of the great arteries as determined by micro MRI scans of E14.5 embryos

3D reconstruction of high resolution MRI data from E15.5 embryos (Amira® software, Visage Imaging Inc.) showing the great arteries. Ventral (left) and dorsal (right) views are shown for each genotype indicated. Individual structures are coloured as follows: orange for the aortic arch and descending aorta, purple for the pulmonary artery, the trachea is highlighted in white and the heart is shaded in brown with the right ventricle in blue and the left ventricle in red. Where there is a ventricular septal defect (VSD), both ventricles are in red. Arteries are labelled as LSA: Left Subclavian Artery, LCA: Left Common Carotid

NIH-PA Author Manuscript

NIH-PA Author Manuscript

NIH-PA Author Manuscript

Artery, RSA: Right Subclavian Artery, RCA: Right Common Carotid Artery and DA: Descending Aorta.

A) *Spry1+/-;Spry2+/-* control embryo and (B) *Tbx1+/-* embryo with normal arteries and normal heart.

C, D) Examples of *Spry1+/-;Spry2+/-;Tbx1+/-* embryos with normal vessels (C) or retroesophageal aortic arch (REAA) and aortic vascular ring (D).

E,G,I) Compound *Spry1;Spry2* mutant embryos with normal anatomy.

F) *Spry1+/-;Spry2-/-;Tbx1+/-* embryo with normal arteries and a ventricular septal defect (VSD, indicated by an arrow). Both ventricles are coloured in red to indicate mixing of oxygenated and de-oxygenated blood due to the VSD.

H) *Spry1-/-;Spry2+/-;Tbx1+/-* embryo with REAA.

J) Spry1-/-;Spry2-/-;Tbx1+/- embryo with interrupted aortic arch type B (IAA-B).

NIH-PA Author Manuscript
NIH-PA Author Manuscript
NIH-PA Author Manuscript

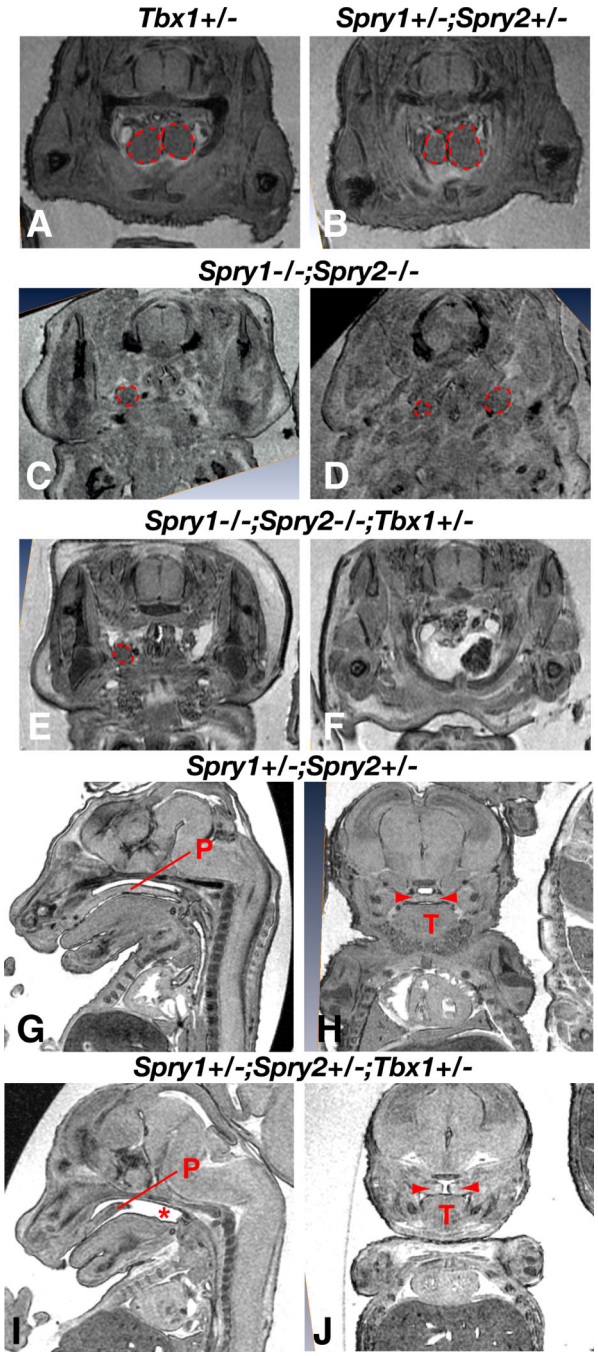

Figure 5. Genetic interaction between Sprouty and Tbx1 genes during thymus and palatal development

A-F) MRI sections through the thoracic region of E15.5 embryos with the thymus lobes outlined in red. Examples of hypoplasia (C,D,E), hypoplasia with ectopia (C,E) and aplasia (F) can be seen.

G-J) Sagittal (G,I) and frontal (H,J) scans through embryonic heads showing a normal palate fused at the midline in a *Spry1+/-;Spry2+/-* embryo (G,H) and a cleft palate in a *Spry1+/-;Spry2+/-;Tbx1+/-* embryo (I,J).

NIH-PA Author Manuscript
NIH-PA Author Manuscript
NIH-PA Author Manuscript

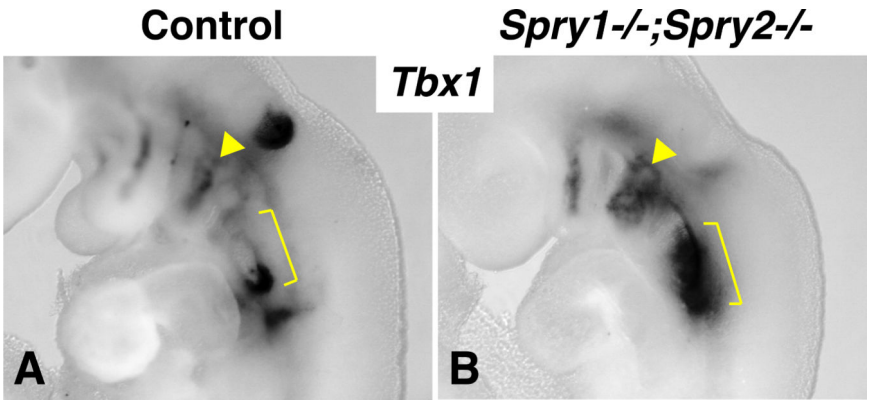

Figure 6. Expanded Tbx1 expression in Sprouty-deficient embryos

In situ hybridisation for *Tbx1* mRNA in E9.5 control (A) and *Spry1-/-;Spry2-/-* (B) embryos are compared. Note the expanded *Tbx1* expression in the second pharyngeal arch (yellow arrowhead) and caudal arches (yellow bracket) in the mutant embryo.

NIH-PA Author Manuscript
NIH-PA Author Manuscript
NIH-PA Author Manuscript

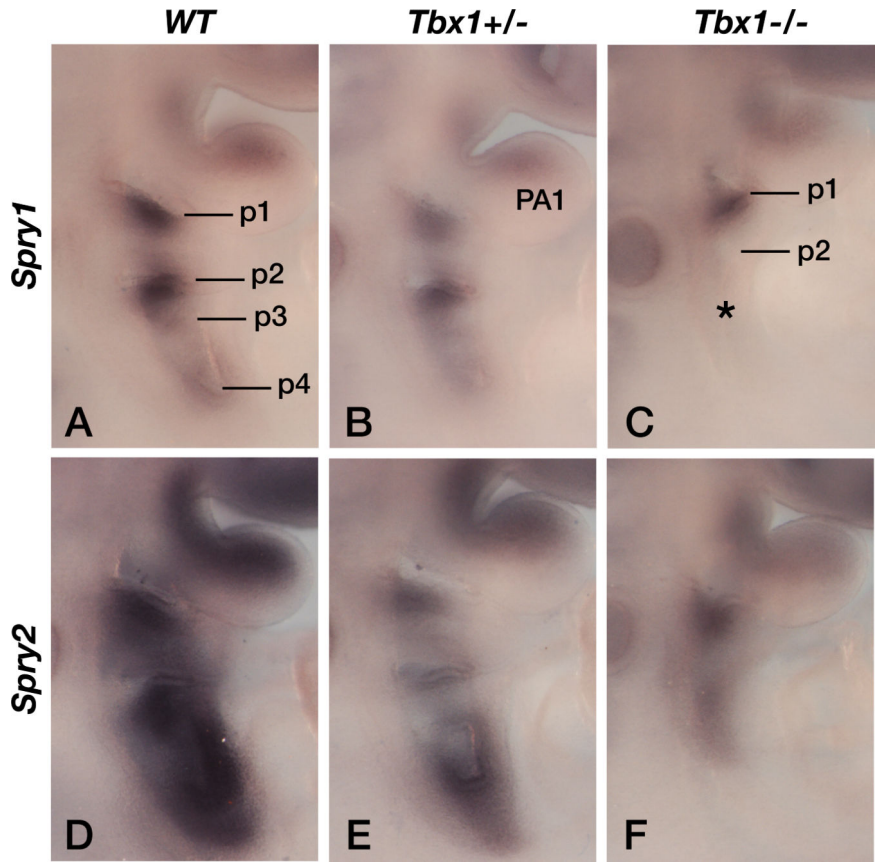

Figure 7. Reduced RTK signaling as measured by Sprouty gene expression in Tbx1-deficient embryos

A-C) *Spry1* gene expression in somite stage-matched E9.5 wildtype (WT), *Tbx1+/-* and *Tbx1-/-* embryos. Pharyngeal pouches (p1-p6) and the first pharyngeal arch (PA1) are labeled.

D-F) *Spry2* gene expression in somite stage-matched E9.5 wildtype (WT), *Tbx1+/-* and *Tbx1-/-* embryos.

NIH-PA Author Manuscript
NIH-PA Author Manuscript
NIH-PA Author Manuscript

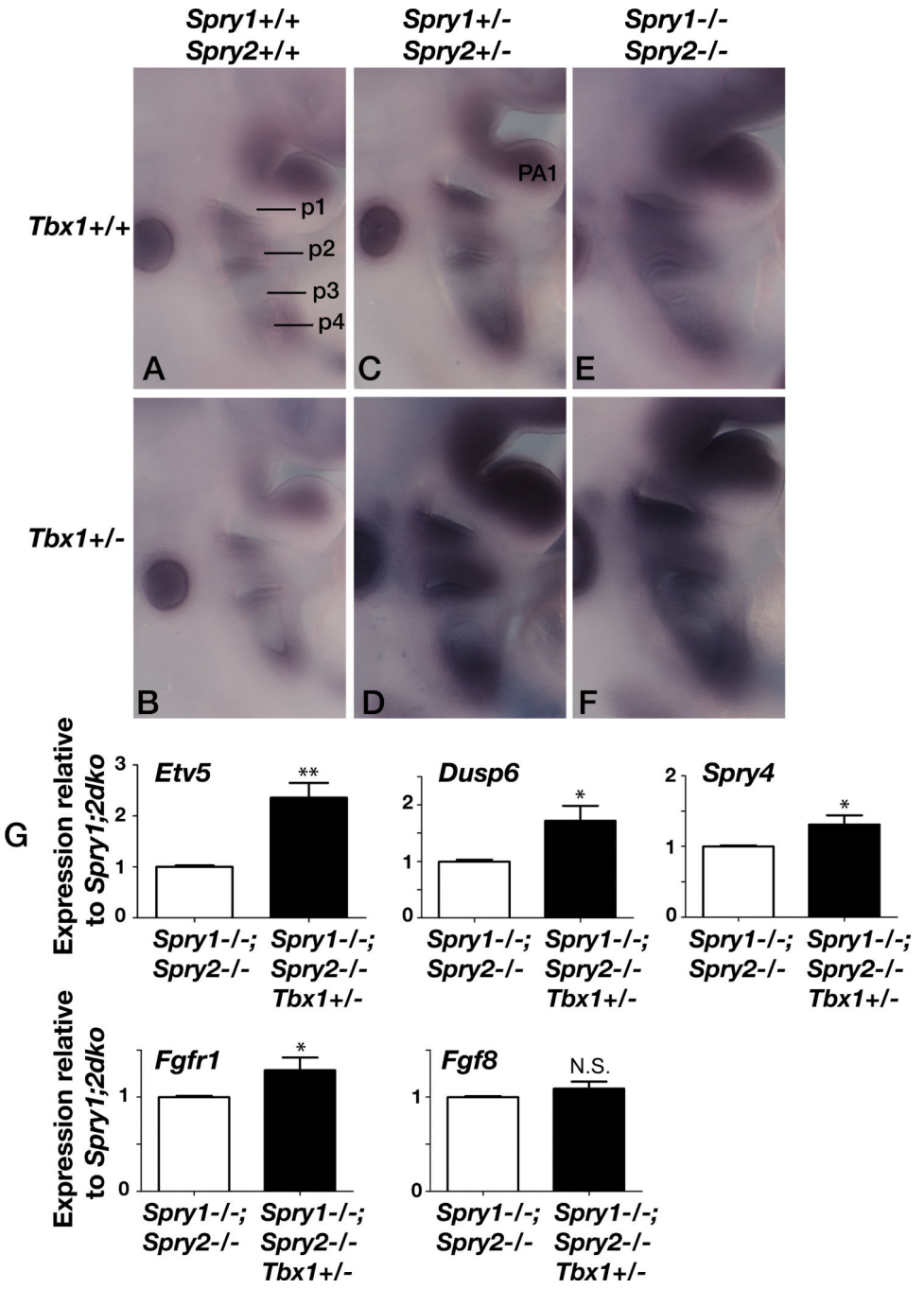

Figure 8. Deregulated RTK signaling as measured by Etv5 (Erm) gene expression in Sprouty; Tbx1 -deficient embryos

Comparative images of the pharyngeal region of somite-matched E9.5 embryos after *in situ* hybridization for *Etv5*. Hybridisations were performed simultaneously under identical conditions and at least two independent experiments gave similar results. Pharyngeal pouches (p1-p4) and the first pharyngeal arch (PA1) are labeled. Note the slight reduction in *Etv5* expression in B, compared to A, especially in PA1, the gradual increase in *Etv5* expression as more Sprouty alleles are deleted (compare A, with C, with E), and the

NIH-PA Author Manuscript

NIH-PA Author Manuscript

NIH-PA Author Manuscript

pronounced upregulation in *Tbx1*+/- embryos (D,F) compared to *Tbx1*+/+ embryos with the same Sprouty genotype (C,E).

G) Quantitative RT-PCR analysis of RTK target gene (*Etv5*, *Dusp6* and *Spry4)* expression in the pharyngeal apparatus isolated from *Spry1-/-;Spry2-/-* and *Spry1-/-;Spry2-/-;Tbx1*+/- embryos (as in E and F) are shown. Quantitation of *Fgfr1* and *Fgf8* transcripts are also shown. Expression levels are represented as relative to those in *Spry1-/-;Spry2-/-* (*Spry1;2dko*) embryos. *p<0.05; **p<0.01; N.S. = no significant difference.

NIH-PA Author Manuscript
NIH-PA Author Manuscript
NIH-PA Author Manuscript

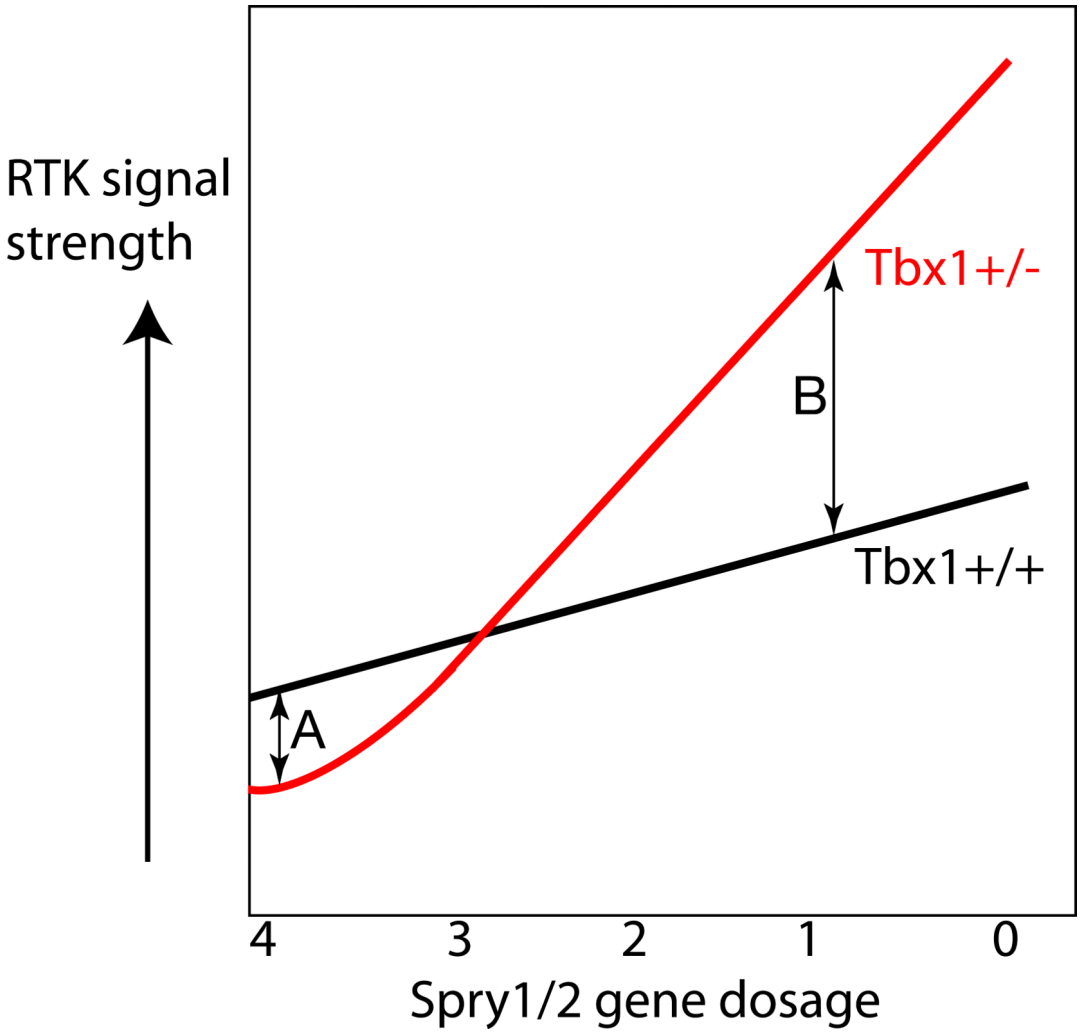

Figure 9. Diagrammatic representation of the effects of Tbx1 haploinsufficiency on RTK signal strength as a function of Sprouty gene dosage

In embryos with a wild-type complement of *Spry1/2* gene dosage (4 wildtype alleles), *Tbx1*+/- embryos show reduced levels of FGF signalling in the pharyngeal apparatus compared to *Tbx1*+/+ embryos, presumably due to the downregulation of FGF ligands in different tissues (A). As Sprouty gene dosage is reduced in *Tbx1*+/+ embryos, the level of RTK signalling increases due to the loss of RTK antagonists (black line). The level of RTK signalling increases disproportionally in *Tbx1*+/- embryos (red line), suggesting that normal TBX1 levels is required to buffer or protect the pharyngeal apparatus from increased RTK signaling (B).

NIH-PA Author Manuscript

NIH-PA Author Manuscript

NIH-PA Author Manuscript

Table 1

Sprouty/Tbxl interactions during development of the palate

Spry1	Spry2	*Tbx1*	n	Cleft palate
	+/+	+/−	3	0
+/−	+/−	+/+	2	0
		+/−	21	8*
−/−	+/−	+/+	4	4
		+/−	16	14
+/−	−/−	+/+	6	6
		+/−	15	14
−/−	−/−	+/+	3	3
		+/−	7	7

Shaded cells indicate significant difference between Tbx1 +/+ and Tbx1 +/− embryos:

* p=0.03

NIH-PA Author Manuscript

NIH-PA Author Manuscript

NIH-PA Author Manuscript

Table 2

Sprouty/Tbxl interactions during thymus development

Spry1	Spry2	*Tbx1*	n	Normal	Hypoplasia	Hypoplasia with ectopia	Aplasia	TOTAL
+/+	+/+	+/−	35	28	7	0	0	7
+/−	+/−	+/+	23	23	0	0	0	0
		+/−	35	32	3	0	0	3
−/−	+/−	+/+	20	18	1	1	0	2
		+/−	35	30	2	1	2	5
+/−	−/−	+/+	13	13	0	0	0	0
		+/−	24	9	**9***	1	5	**15****
−/−	−/−	+/+	7	0	0	7	0	7
		+/−	16	0	5	0	**11*^**	16

Shaded cells indicate significant difference between Tbx1+/+ and Tbx1+/− embryos:

* p=0.015

** p=0.0002

*^ p=0.005

NIH-PA Author Manuscript

NIH-PA Author Manuscript

NIH-PA Author Manuscript

Table 3

Sprouty/Tbx1 interactions during cardiovascular development

				E10.5[a]			E15.5-E17.5[b]		
Spry1	**Spry2**	***Tbx1***	**n**	**1st PAA**	**PAA**	**PAA**	**Aortic arch**	**OFT defects**	**VSD**
+/+	+/+	+/+	21	0	0	0	nd	nd	nd
		+/−	17	1	0	0	0/38	0/38	1/17
+/−	+/−	+/+	8	0	0	0	0/30	0/30	0/3
		+/−	14	1	0	**7***	4/38	0/38	0/19
−/−	+/−	+/+	10	0	0	1	0/20	0/20	0/9
		+/−	22	1	1	**17****	**9/33****	0/33	0/23
+/−	−/−	+/+	10	1	2	0	0/13	0/13	0/10
		+/−	14	0	2	**7***	**8/29****^	0/30	5/19
−/−	−/−	+/+	16	0	**6**^	**5**^^	0/11	0/11	2/8
		+/−	12	**5****	**10***	**10*****	**12/16*****	2/16	4/10

Aortic arch defects were scored at E10.5 by India ink injections (a) or at later stages by MRI or histology (b).

Outflow tract (OFT) defects and Ventricular Septal defects (VSD) were also scored in E15.5-E17.5 embryos.

Significant incidence compared to wildtype controls (Fisher's exact test, two tailed):

Shaded cells indicate a significant difference between *Tbx1*+/+ and *Tbx1*+/− embryos:

^ p=0.003

^^ p=0.01

* p=0.02

** p=0.01

**^ p=0.04

*** p<0.001